Published in final edited form as:
Mech Dev. 2007 ; 124(9-10): 682–698. doi:10.1016/j.mod.2007.07.003.

Zebrafish *colgate/hdac1* functions in the non-canonical Wnt pathway during axial extension and in Wnt-independent branchiomotor neuron migration

Roopa M. Nambiar, **Myron S. Ignatius**, and **Paul D. Henion***
Center for Molecular Neurobiology Molecular, Cell and Developmental Biology Program Department of Neuroscience Ohio State University 105 Rightmire Hall, 1060 Carmack Rd. Columbus, OH 43210

Abstract

Vertebrate gastrulation involves the coordinated movements of populations of cells. These movements include cellular rearrangements in which cells polarize along their medio-lateral axes leading to cell intercalations that result in elongation of the body axis. Molecular analysis of this process has implicated the non-canonical Wnt/Frizzled signaling pathway that is similar to the planar cell polarity pathway (PCP) in *Drosophila*. Here we describe a zebrafish mutant, *colgate (col)*, which displays defects in the extension of the body axis and the migration of branchiomotor neurons. Activation of the non-canonical Wnt/PCP pathway in these mutant embryos by overexpressing Δ*Ndishevelled*, *rho kinase2* and *van gogh-like protein 2 (vangl2)* rescues the extension defects suggesting that *col* acts as a positive regulator of the non-canonical Wnt/PCP pathway. Further, we show that *col* normally regulates the caudal migration of nVII facial hindbrain branchiomotor neurons and that the mutant phenotype can be rescued by misexpression of *vangl2* independent of the Wnt/PCP pathway. We cloned the *col* locus and found that it encodes *histone deacetylase1 (hdac1)*. Our previous results and studies by others have implicated *hdac1* in repressing the canonical Wnt pathway. Here, we demonstrate novel roles for zebrafish *hdac1* in activating non-canonical Wnt/PCP signaling underlying axial extension and in promoting Wnt-independent caudal migration of a subset of hindbrain branchiomotor neurons.

Keywords

Wnt signaling; histone deacetylase; convergent extension; migration; PCP; zebrafish

Introduction

The basic vertebrate body plan consists of the three germ layers that emerge during gastrulation. Carefully orchestrated movement of groups of cells relative to each other culminates in the transformation of an unstructured mono-layered blastula into a gastrula with germ layers. Cell intercalations result in the elongation of the body axis. An important driving force for these cell movements is a process known as convergent-extension (CE). Studies suggest that CE in zebrafish has at least two distinct components (Kane and Warga, 1994; Solnica-Krezel et al.,

*author for correspondence: e-mail: E-mail: henion.1@osu.edu), Center for Molecular Neurobiology, Ohio State University, 105 Rightmire Hall, 1060 Carmack Rd,. Colombus, OH 43210, Ph 614-292-5111\Fax 614-292-5379.

1995; Wallingford et al., 2002). The first involves directed migration of cells towards the dorsal side of the gastrula, termed dorsal convergence. Convergence is a migratory event not involving cell rearrangements. This is followed by cellular rearrangements where cells converging at the dorsal midline become polarized along the medio-lateral axis resulting in cell intercalations and elongation of the body axis.

The dissociation of convergence and medio-lateral intercalation and extension is evident from zebrafish mutants affecting CE movements differently. For example, in *silberblick (slb)* mutants, both convergence and extension movements are defective (Heisenberg et al., 2000), whereas in *no tail (ntl)* and *somitabun (sbn)* mutants convergence is significantly affected with extension occurring almost normally (Myers et al., 2002; Solnica-Krezel et al., 1996). In *knypek (kny)* mutants, mediolateral intercalations that underlie CE movements are impaired (Topczewski et al., 2001).

The molecular basis for CE movements in vertebrates is incompletely understood. The polarization of cells within the plane of tissues undergoing CE in vertebrate embryos is akin to the polarization of epithelial cells in the insect cuticle. In *Drosophila*, the orientation of cells in a plane, planar cell polarity (PCP), is regulated by a non-canonical Wnt signaling cascade. As in the case of the canonical Wnt signaling pathway, this pathway also uses the Frizzled receptor and Dishevelled (Dsh). Other proteins, such as Inversin, (Simons et al., 2005), Diversin, (Schwarz-Romond, 2002), Naked and Casein Kinase 1 (Yan et al, 2001; McKay et al., 2001), all of which either interact directly with Dsh or with Dsh-associated proteins, have been shown to regulate both Wnt pathways. However, downstream of Dsh, PCP signaling recruits a different set of molecules including Van gogh-like protein 2, Prickle, and JNK (Shulman et al, 1998; Boutros and Mlodzik, 1999; Adler and Lee, 2001).

Recent studies have revealed that the orthologs of PCP pathway molecules control CE during gastrulation in *Xenopus* and zebrafish (Park and Moon, 2002; Kibar et al., 2001; Carreira-Barbosa et al., 2003). Mutant versions of Dsh have implicated the PCP signaling pathway as a regulator of CE movements in vertebrates (Heisenberg et al., 2000; Tada and Smith, 2000; Wallingford et al., 2000). A construct of Dsh that specifically disrupts PCP signaling in *Drosophila*, but does not affect the canonical Wnt pathway was able to block CE movements in both *Xenopus* and zebrafish (Wallingford et al., 2000; Heisenberg et al., 2000). Conversely, deletion constructs of Dsh that are unable to activate the canonical Wnt pathway were shown to rescue CE in *silberblick*, a zebrafish *wnt11* mutant, as well as the overexpression of a dominant-negative form of *wnt11* in *Xenopus* embryos (Tada and Smith, 2000; Heisenberg et al, 2000). In addition to *dsh*, other PCP genes also have homologs in vertebrates. For example, the zebrafish *trilobite* mutant is defective in the homolog of the *van gogh-like protein 2* gene and is expressed in cells undergoing CE (Park and Moon, 2002). Two homologs of *prickle* that regulate gastrulation movements in zebrafish have been identified recently (Veeman et al., 2003; Carreira-Barbosa et al., 2003). Additionally, other CE genes specific to vertebrates have been isolated, including the *formin* morphology protein *daam-1, knypek/glypican 4/6* and Wnt ligands *wnt5/pipetail* and *wnt11/silberblick* (Hammerschmidt et al., 1996; Heisenberg et al., 2000; Jessen et al., 2002; Kilian et al., 2003; Rauch et al., 1997; Solnica-Krezel et al., 1996; Topczewski et al., 2001).

Chromatin modifications play a key role in regulating eukaryotic gene expression (Jenuwein and Allis, 2001). Histones have numerous sites where post-translational modifications occur, and the pattern of modification encodes the expression status of a gene (Strahl and Allis, 2000; Rice and Allis, 2001). The silencing of gene expression has been found to be associated with deacetylation whereas acetylation of histones is associated with activation of gene expression (Allfrey, 1966). Histone deacetylases (HDACs) are primarily nuclear enzymes involved in removing acetyl groups from histone lysine tails (de Ruijter et al., 2003; Marks et

al., 2003). A role for Hdac1 in repressing the expression of canonical Wnt target genes has been shown in *Drosophila* and vertebrates (Chen et al., 1999; Billin et al., 2000; Brantjes et al., 2001; Yamaguchi et al., 2005). Hdac1 has been shown to exert its repressive function via association with Groucho and LEF1 in the nucleus (Chen et al., 1999; Brantjes et al., 2001; Billin et al., 2000). Roles for zebrafish *hdac1* in *notch* and *sonic hedgehog* signaling have also been reported (Yamaguchi et al., 2005; Cunliffe, 2004).

We have shown that the zebrafish mutant *colgate (col)* displays defects in early dorso-ventral and brain patterning (Nambiar and Henion, 2004) that can exclusively be rescued by overexpression of canonical Wnt pathway antagonists (Nambiar and Henion, 2004). Here, we show that *col* mutants also display defects both in axial extension and the migration of a subset of hindbrain branchiomotor neurons that can be selectively and differentially rescued by overexpressing molecules of the non-canonical Wnt/PCP signaling pathway. We have cloned the *col* locus and found that it encodes *histone deacetylase 1 (hdac1*). In this study we demonstrate novel roles for Hdac1 in the non-canonical Wnt/PCP pathway during axial extension as well as in Wnt/PCP-independent neuronal migration, functions not previously attributed to *hdac1*.

Materials and Methods

Fish strains

Adult zebrafish and embryos were maintained at 28.5 C and staged by hours post fertilization (hpf), days post fertilization (dpf) or morphological criteria (Kimmel et al., 1995). Mutant embryos (*AB and WIK background) were collected from pair-wise matings of heterozygous adults. All phenotypic analyses of *col* mutants were done using embryos homozygous for the *col* ^{b382} allele (Henion et al., 1996).

Axis length, somite number and notochord diameter measurements

To compare axis length between *col* mutant and wildtype embryos (Table 1), images of wild-type and *col/hdac1* mutant embryos were taken at identical positions under a Leica compound light microscope and then measurements were made using the Leica SPOT v 4.0 software measurement tools that were calibrated with a standard stage micrometer. 20 wild-type and 20 *col/hdac1* mutants were used for analysis at 25 hpf and 10 each of wild-type and *col/hdac1* mutant embryos were measured at 48 hpf and 72 hpf. The data obtained was analyzed using 2 way ANOVA and Bonferroni post hoc tests. Graph prism pad version 4.0 software was used to conduct statistical analysis and graph data.

Quantification of somite numbers in time-matched (hpf) *col* mutant and wildtype embryos was performed at 16hpf, 27hpf and 48hpf (Table 2). Embryos were obtained from *col* heterozygous adults. Somite pairs of a clutch of live individual embryos at 16hpf were counted within 25 minutes and the embryos were allowed to develop to 27hpf when the *col* phenotype is readily apparent in order to assign genotype to individual embryos. For counts at 27hpf and 48hpf, embryos were anaesthetized with tricaine to immobilize them for counts.

For notochord diameter quantification (Table 3),10 embryos of each type (wildtype uninjected, *col* uninjected, Δ*Ndsh* injected *col* and wildtype, *rok2* injected *col* and wildtype and *vangl2* injected *col* and wildtype) at 48 hpf were fixed and labeled with f59 antibody to provide tissue contrast. Embryos were cryosectioned (16 μm) and 6–7 mid-trunk sections per embryo were imaged. The images were then transferred to a drawing program (Adobe Photoshop 7.0) and notochord measurements were made using the scale bar. The significance of differences from observed values was assessed using the Mann-Whitney U test. The increase in notochord diameter observed in *col* mutants compared to wildtype was found to be significant, $p<0.002$.

Because no significant differences were observed between uninjected wildtype and all injected wildtype embryos, these data are not shown (see Results).

Trichostatin A treatment

Trichostatin A (TSA; Biovision Research Products) was dissolved in DMSO at a concentration of 1mg/ml. This stock solution was then diluted in fish water to the concentrations indicated.

Genetic mapping and cloning

For linkage analysis, AB background heterozygous *col* individuals were crossed to a polymorphic WIK strain and mutant and wild type embryos were used. Genomic DNA was prepared from 1534 embryos and PCR was performed using Simple Sequence Length Polymorphic markers (SSLP; Knapik et al., 1996). Primer sequences for SSLP markers were obtained from the MGH zebrafish database. The *ck2b*, *hdac1* and *hey1* coding sequences were amplified from *col* ^{b382} by RT-PCR and then directly sequenced. A single nucleotide polymorphism (T to A) at position 583 in the *ck2b* cDNA sequence was used to identify recombinants. The CHORI211 BAC library was screened by PCR using the *ck2b* primers to identify positive BAC clones. BAC end sequences were obtained from the Sanger Institute database (http://trace.ensembl.org) and PCR primers were designed to amplify regions of these sequences from mutant and wildtype embryos. Polymorphisms were identified in these amplicons and used to check for recombinants. The splice site lesion was identified from several independently amplified fragments from *col* and wildtype genomic DNA using PCR primers (5′-TAACGTAGGGGAGGATTGTC- 3′) and (5′-CAGCTCCAGAATGGCCAGTAC- 3′) that amplify across intron 4–5. Mutant and wildtype spice variants were examined using RT-PCR.

Plasmid constructs

The full-length *hdac1* gene cloned into pBS SK+ was a gift from I. Masai (RIKEN, Japan). Other constructs used in this study were *vangl2/tri* (Jessen et al., 2002), *rho kinase 2*(Jessen et al., 2002), Δ*N dsh* (Heisenberg et al., 2000). In situ probes for *hdac1* were generated using the first 720 bp of the *hdac1* cDNA and cloning into the TOPO TA vector. Probes were synthesized by digesting with Pvu I followed by transcription using T7 polymerase.

mRNA and morpholino injections

mRNA was synthesized using Ambion's T7, T3 or SP6 mMessage mMachine kit (Ambion). Following transcription, the mRNA was extracted using phenol/chloroform and concentrated in Microcon YM-50 (Amicon) microconcentrator filter devices. RNA quality was assayed using gel electrophoresis. mRNA was diluted in 1% phenol red and pressure injected into the YSL of 1 to 8-cell stage embryos. The concentration of RNA injected into each embryo was approximately 50–500pg depending on the RNA used.

The antisense *hdac1* morpholino was targeted to the translational initiation site (5′-TTGTTCCTTGAGAACTCAGCGCCAT -3′) and a modified morpholino was also used as a specificity control (5′-TTGcTCCcTGAGAtCTCAGgGCCAT-3′). The sequence for the MO targeting *vangl2* was the same as Park and Moon, 2002. All morpholinos were obtained from Gene Tools. The morpholinos were diluted with phenol red/0.2M KCl (1:6) prior to injection and 2–8 ng was injected per embryo. Morpholinos were pressure injected into the YSL of 1 to 8-cell stage embryos.

In situ hybridization, immunohistochemistry and genotyping

In situ hybridization was performed using standard protocols. The following probes were used: *no tail* (Schulte-Merker et al., 1992), *foxd3* (Odenthal and Nusslein-Volhard, 1998), *vangl2*

(Park and Moon, 2002), *myod* (Weinberg et al., 1996), *islet1* (Korzh et al., 1993), *dlx2* (Akimenko et al., 1994), *wnt5a* (Rauch et al., 1997), *krox20* (Wilkinson et al., 1989), *val* (Moens et al., 1996), *huC* (Kim et al., 1996), *hoxb3* (Prince et al., 1998), *wnt11* (Heisenberg et al., 2000), *wnt8* (Kelly et al., 1995). Probes were synthesized using T7, T3 or SP6 RNA polymerases and DIG labeled rNTPs as appropriate. For in situ hybridizations on embryos older than 24 hpf, the embryos were raised in 0.03g/l 1-phenyl-2-thiourea (PTU) to prevent melanin synthesis which allowed clear analysis of gene expression patterns without interference from pigmented melanophores.

Immunohistochemistry was performed according to Henion et al., 1996. The antibodies used were F59 (Crow and Stockdale, 1986), zn12 (Trevarrow et al., 1990), acetylated tubulin (Sigma), RMO44 (Zymed) and actin (Abcam).

To determine the genotype of embryos used in experiments before a readily apparent phenotype is seen, DNA from individual embryos was obtained and PCR was performed on genomic DNA using the closely linked SSLP marker Z7235.

Results

Defects in axial extension contribute to the *col* mutant phenotype

col mutant embryos are shorter (Table 1) and have a downward curved body compared to wildtype embryos. The somites of 48 hpf *col* mutants appear rounded, unlike chevron-shaped wildtype somites (Fig. 1A, B). There are also fewer somite pairs in *col* mutants than in wildtype by 27hpf, although no significant difference is apparent at 16hpf (Table 2). The 1–2 somite pair deficit in *col* mutants at 27hpf persists at 48hpf (Table 2). Compared to wildtype embryos, *col* mutants also have abnormally wide and stunted notochords (Fig. 1A-D) with defects being prominent by 30 hpf. Quantification of notochord diameter in transverse sections of the trunk of *col* mutants and wildtype siblings at 48 hpf revealed that notochord diameter was significantly larger (15%; Table 3; see Materials and Methods) in mutants (Fig.1C, D). Notochord specification and early somite development, however, appear overtly normal in *col* mutants as expression of *ntl* and *myoD* in embryos at late gastrulation (Fig. 1E, F; not shown) and at early somitogenesis (not shown) is similar to that of wildtype embryos. Likewise, neurulation and lengthening of the neural keel as evidenced by the expression of *foxd3* (Fig. 1G, H) and *huC* (not shown) during early somitogenesis appears unaffected. It is nevertheless possible that subtle early defects are present and become accentuated over time during morphogenesis. This temporal pattern of phenotypic changes has been documented previously for anteroposterior brain patterning in *col* mutants (Nambiar and Henion, 2004).

The components of the axis extension phenotype of *col* mutants described above are reminiscent of, although much less pronounced than, those observed in the zebrafish Wnt/PCP mutants *silberblick* and *trilobite* as well as *prickle* morphants (Heisenberg et al., 2000; Sepich et al., 2000; Carreira-Barbosa et al., 2003), suggestive of a defect in extension movements as a result of the *col* mutation.

col mutant embryos display defects in the migration of hindbrain branchiomotor neurons

The branchiomotor neurons are born in specific rhombomeres in the hindbrain and innervate muscles of the pharyngeal arches (Noden, 1983; Chandrasekhar et al., 1997). In zebrafish the facial (nVII) and the glossopharyngeal (nIX) motor neurons migrate tangentially to their final destinations (Chandrasekhar et al., 1997). The trigeminal or nV neurons are specified as discrete clusters in r2 and r3. These two clusters of neurons are functionally distinct that can be attributed to the segmental origin of the motor neurons (Higashijima et al., 2000). At 21 hpf most of the facial (nVII) neurons are localized in r4 and r5, as judged by comparison to the

otocyst. In the next 15 hrs the nVII motor neurons migrate tangentially such that by 36 hpf most of these neurons are located in r6 and r7.

In *trilobite/vangl* mutants, nVII and nIX neurons do not migrate into caudal rhombomeres following induction in r4 and r6 respectively (Bingham et al., 2002). Defects in the migration of these motor neurons are not a consequence of defective hindbrain patterning or widespread cell migration defects. Although *tri/vangl* mutants also display abnormal CE movements during gastrulation, the neuronal migration defect is not a consequence of gastrulation-associated cell movement abnormalities (Bingham et al., 2002). Similar defects are also observed in *pk1*morphants (Carreira-Barbosa et al., 2003).

We have found that *col* mutants display a branchiomotor neuron migration phenotype reminiscent of *tri/vangl* mutants and *pk1* morphants. Specifically, the facial (nVII) neurons identified by *islet-1*mRNA and Islet1 protein expression fail to migrate caudally and remain in r4 (Fig. 2). Like in the case of *vangl2* mutants, we observed that the general development of the hindbrain in *col* mutants is largely unaffected. The expression of the markers *krox20*, *valentino* and *hoxb3* that are diagnostic for r3, 5 and 6 development, respectively, were comparable between wildtype and *col* mutant embryos (Fig. 3A-F). Also, the patterning of other hindbrain neuronal populations such as hindbrain commissural and reticulo-spinal neurons, as identified by staining with acetylated tubulin (not shown) and RMO44 antibodies respectively, was generally unaffected in *col* mutants (Fig. 3G, H). However, the number of neurons appeared to be reduced in number in *col*. These results suggest that the failure of facial (nVII) neuronal migration is specific to these neurons and not due to a general defect in hindbrain patterning.

Canonical and non-canonical Wnt pathway phenotypes of *col* mutants are genetically distinguishable

The embryonic patterning (Nambiar and Henion, 2004) and extension defects in *col* mutant embryos suggest a role for *col* in both canonical Wnt and non-canonical Wnt/PCP signaling. Therefore, we sought to determine the role of *col* in both arms of the Wnt signaling cascade. Injection of antagonists of the canonical pathway including *dkk1*, *gsk3β* and *wnt8* MO, all resulted in the rescue of canonical pathway phenotypes of *col* mutants (Nambiar and Henion, 2004). In contrast, these canonical pathway antagonists failed to rescue the extension defects in *col* mutants (Nambiar and Henion, 2004; not shown). In addition, injection of the BMP inhibitor *chordin* mRNA and *XFD*, an FGF pathway antagonist also failed to rescue the extension defects in col embryos Nambiar and Henion, 2004; not shown). The persistence of extension defects in *col* mutants in which the patterning phenotypes were rescued is consistent with a role for *col* in regulating non-canonical as well as canonical Wnt signaling.

In order to delineate a potential role of *col* in the Wnt/PCP pathway, we first examined the expression of two *wnt* genes, *wnt11* and *wnt5a*, both of which are known to play roles in regulating CE movements in vertebrates, including zebrafish (Heisenberg et al., 2000; Rauch et al., 1997). The overall patterns of embryonic expression of both genes were indistinguishable between *col* mutants (identified by genotyping with flanking marker Z9059) and wildtype embryos, except for an increase in *wnt5a* expression in the tailbud (not shown). This increased expression can be attributed to the accumulation of cells in the tailbud region as revealed by the expression of other markers such as *ntl* and *wnt8* (Nambiar and Henion, 2004). Although we cannot rule out the existence of subtle changes, the generally unaltered expression of *wnt5a* and *wnt11* in *col* mutants is consistent with a potential role of *col* in regulating the Wnt/PCP pathway independently of *wnt5a* and/or *wnt11*.

To further test whether *col* functions in the Wnt/PCP pathway, misexpression experiments were performed with regulatory components of the vertebrate Wnt/PCP pathway. *dshΔN*, a

dsh construct lacking the N-terminal end that has been shown to activate the Wnt/PCP pathway and rescue CE defects in *slb* mutants (Heisenberg et al., 2000) and *rho kinase2* RNA, which also activates the Wnt/PCP pathway (Marlow et al., 2002), were injected into embryos at 1–8 cell stage. We injected each of these RNAs independently into wildtype embryos and found that in the vast majority of individual embryos misexpression did not result in an abnormal phenotype, although a small number of injected embryos displayed variable defects in the morphogenesis of the prechordal plate and notochord (not shown). Misexpression of either RNA construct in homozygous *col* mutant embryos resulted in qualitatively equivalent suppression of the axial extension defects present in uninjected mutants (Fig. 4A-F). Injected mutant embryos (*dsh*Δ*N* 90%, n=50; *rok2* 90%, n=82; Table 4) displayed significantly longer, extended body axes (Fig. 4A-C) and their notochords were thinner (Table 3) and longer compared to uninjected mutants (Fig. 4D-F). *dsh*Δ*N* and *rok2* injected *col* mutants retained defects in the canonical Wnt signaling pathway as evidenced by persistent brain patterning defects including, for example, reduced *dlx2* expression in the anterior forebrain (Fig. 4G-I and not shown). Homozygous *col* mutants in all cases were identified by genotyping with flanking marker Z9059. These results strongly suggest that *col* functions in the regulation of the non-canonical/PCP pathway as well as in the canonical Wnt signaling pathway.

The non-canonical Wnt/PCP pathway regulator *vangl2* rescues defects in extension as well as branchiomotor neuron migration in *col* mutants

Although overexpression of *dsh*Δ*N* and *rho kinase2* RNAs rescue axial extension defects in *col* mutants, branchiomotor neuron migration remains defective in injected mutants with cell bodies remaining in r4 in injected *col* mutants (not shown). However, another Wnt/PCP pathway regulator, *van gogh-like protein 2 (vangl2)*, is known to be required for both CE movements in the gastrula and branchiomotor neuron migration (Bingham et al., 2002). We therefore tested the effects of *vangl2* misexpression in *col* mutants on both axis extension and branchiomotor neuron migration. Injection of *vangl2* RNA into *col* mutant embryos resulted in embryos with extended body axes and longer, thinner notochords when compared to uninjected mutants (Fig. 5A-D; Tables 3 and 4). Additionally, in *vangl2* injected *col* mutants, facial branchiomotor neurons identified by *islet-1* expression migrate from r4 to r6 and r7 in a pattern indistinguishable from wildtype embryos in 80% of injected mutants (Fig. 5A-C; Table 4). As was the case upon overexpression of *dsh*Δ*N* and *rho kinase2* RNAs in *col* mutants (Fig. 4G-I), canonical Wnt signaling-dependent neural patterning defects remain defective in *vangl2* injected *col* mutants (not shown). Phenotypic rescue of the extension defects in *col* mutants by *vangl2* misexpression provides further evidence for the involvement of *col* in the regulation of the non-canonical/PCP pathway. In contrast, the rescue of branchiomotor neuron migration in *vangl2* injected *col* mutants demonstrates an additional genetic interaction between *col* and *vangl2* and indicates a novel role for *col* that is independent of Wnt signaling pathways.

The *col* locus encodes *histone deacetylase 1*

The col^{b382} mutation was mapped to LG19 (Nambiar and Henion, 2004). Using SSLP markers it was placed approximately 0.6cM south of Z9059 (6 recombinants out of 1004) and 1.6cM north of Z22532 (17 recombinants out of 1004). An examination of the annotated genes between Z9059 and Z22532 revealed that the zebrafish orthologs of *casein kinase 2b (ck2b)*, *histone deacetylase1 (hdac1*) and *hairy/enhancer-of-split related with YRPW motif1 (hey1)* lie within this interval (Fig. 6A). The roles of *ck2b* and *hdac1* as negative regulators of canonical Wnt signaling have been established (Dominguez et al., 2004; Willert et al., 1997; Billin et al., 2000; Yamaguchi et al., 2005) prompting us to sequence the cDNAs of these genes. We also sequenced cDNA of the *hey1* gene that lies within the same critical region. The sequencing of *ck2b* and *hey1* cDNAs revealed no lesions. In order to completely rule out *ck2b*, we used a SNP in the gene to identify recombinants. We found two recombinants out of 1024 genomes.

Using the *ck2b* primers we screened a bacterial artificial chromosome (BAC) library. We identified SNPs in the end sequences of two of the BACs, K206D2 and C261D24, and used them as additional markers. Sequencing of the *hdac1* cDNA revealed a 9bp insertion at position 405 resulting in the insertion of 3 amino acids, glutamate, phenylalanine and serine in a conserved motif potentially compromising the structural integrity of the Hdac1 protein. Sequence comparison of *col* mutant and wildtype *hdac1* cDNAs revealed that the wildtype form is absent in *col* mutants (Fig. 6D).

Since a 9 bp insertion is unlikely to result from ENU mutagenesis, we reasoned that the defect could be the result of a point mutation that causes a splicing defect. In order to test this possibility we sequenced *hdac1* from mutant genomic DNA and found a T-to-G transversion in the intron sequence flanking exon 5 that creates a new splice acceptor site (Fig. 6B, C). This results in the addition of 9 bases from the adjacent intron to the 5′ end of exon 5 in *col* mutants.

To determine if the expression pattern of *hdac1* correlates with the development of the *col* mutant phenotype, we analyzed *hdac1* RNA distribution. The *hdac1* gene is ubiquitously expressed from the one cell stage until 18 hpf, suggesting a maternal contribution (not shown). At 24 hpf expression predominates in the brain and eyes and at 2 dpf *hdac1* expression is also seen in the pectoral fin bud, branchial arches and hindbrain (Fig. 6E, G). Our results are consistent to observations by Cunliffe (2004) and Pillai et al (2004). We have shown selective and prominent developmental defects in *col* mutants in all of these regions (Nambiar and Henion, 2004). Overall, *col* mutants do not display a noticeable reduction in the levels of *hdac1* expression (Fig. 6F, H), suggesting that the *col* mutation likely results in impaired Hdac1 protein function due to defective RNA processing

To further test whether the *hdac1* gene is defective in *col* mutants, we assessed the ability of *hdac1* RNA to rescue *col* mutant phenotypes. We found that all characterized phenotypic defects observed in *col* mutants are rescued by *hdac1* RNA injection (85% n=125 Fig. 7; Table 5; Rescued embryos identified by genotyping, see Methods). For example, extension movements are rescued in injected embryos, leading to the development of normally elongated notochords and regular chevron shaped somites (Fig. 7A, C). The forebrain is specified and patterned normally based on the pattern of *dlx2* expression compared to *col* mutants (Fig. 7D, F). Another aspect of phenotypic rescue by *hdac1* RNA injections is the restored migration of branchiomotor neurons and melanophores. Hindbrain branchiomotor facial (nVII) neurons visualized by *islet-1* expression migrate normally into r7 by 33 hpf in injected *col* mutant embryos whereas they fail to migrate out of r4 in uninjected *col* mutants (Fig. 7G, I). Injected *col* mutant embryos displayed the absence of the characteristic cluster of melanophores just posterior to the otic vesicle, a prominent feature of the *col* mutant phenotype (Fig. 7A, C). Lastly, we injected col^{b382}*hdac1* RNA into wildtype embryos and observed no obvious phenotypic consequences (not shown), inconsistent with the possibility of the *col* mutant form of *hdac1* having a dominant-negative activity. We also noted the effects of *hdac1* RNA overexpression in wildtype embryos. Injection of moderate concentrations (400 pg) resulted in a mild reduction of trunk tissue, partial loss of eyes and strikingly, an enlargement of the forebrain (Supplemental Fig. 2A, B). Injection of higher doses (1 ng; 17 0f 20 injected embryos=85%) caused a significant loss of trunk tissue and eyes and a loss of forebrain (Supplemental Fig. 2C, D) and enlargement of midbrain (Supplemental Fig. 2E, F) consistent with our previous data demonstrating that *col* is required for forebrain and midbrain patterning (Nambiar and Henion, 2004). Together, these results suggest that the *col* locus encodes *hdac1* and that the col^{b382} mutation results in a reduction in or loss of *hdac1* activity.

To determine whether *hdac1* knockdown by translational interference in wildtype embryos phenocopies *col* mutants, we injected wildtype embryos with morpholino oligonucleotides (MO) directed to the translational start site of *hdac1*. A large number of embryos injected with

the MO (91.6%; n=120; Table 5) very closely resembled *col* mutants (Fig. 7B, E, H). They were defective in extension movements evidenced by short, curved body axes and thick notochords (Fig. 7A, B). Like *col* embryos, they lacked pectoral fins, retained a cluster of melanophores posterior to the otocyst and displayed grossly truncated anterior brain development (Fig. 7A, B and not shown). These embryos also displayed the reduced domain of *dlx2* expression in the telencephalon (Fig. 7D, E) and migration defect of facial branchiomotor hindbrain neurons expressing *islet-1* (Fig. 7G, H), both characteristic phenotypes of *col* mutants. Embryos injected with the control MO did not show specific defects (not shown).

Taken together, since the *hdac1* gene contains a lesion in *col* mutants, the *col hdac1* gene produces an RNA that is incorrectly spliced, wildtype *hdac1* RNA is able to rescue *col* mutant phenotypes and morpholino-based *hdac1* gene knockdown phenocopies *col* mutants, we conclude that the *col* locus encodes *hdac1*.

col/hdac1 appears to function genetically upstream of *vangl2*

Because *vangl2* misexpression rescues the axial extension and branchiomotor neuron migration phenotypes of *col* mutant embryos, we sought to establish a functional hierarchy between *vangl2* and *col/hdac1*. To do so, we first injected wildtype embryos with *tri/vangl2* MOs. These embryos developed highly stunted body axes with compressed somites and notochords, like *tri* mutants (Supplemental Fig. 1A; Jessen et al., 2002). We then coinjected *hdac1* RNA with the *tri/vangl2* MO in wildtype embryos. We observed that overexpression of *hdac1* RNA was unable to rescue the phenotypes resulting from the injection of *tri/vangl2* MOs (Supplemental Fig. 1B). This result suggests that *hdac1* may be acting genetically upstream of *vangl2* in the Wnt/PCP pathway, although a more detailed analysis is required to define this interaction.

Differential temporal requirements for histone deacetylase activity

To further understand the requirement of histone deacetylase activity in the manifestation of *col* mutant phenotypes, we attenuated HDAC activity in wildtype embryos using the pharmacological agent trichostatin A (TSA), a specific and potent inhibitor of histone deacetylases. TSA inhibits the activity of both type I and type II Hdac proteins by binding to their catalytic domains (Yoshida et al., 1995). We performed two different treatments of embryos with TSA. In the first, we treated wildtype embryos continuously with 50 nM TSA from 5 hpf and fixed embryos at multiple subsequent time points. These embryos displayed specific defects that were more severe than developmental defects in *col* mutant embryos. We observed CE defects in these embryos starting at early somitogenesis (Fig. 8A, B; Table 6). These embryos have shorter, thicker notochords marked by *ntl* expression at the 6-somite stage and 24 hpf (Fig. 8C-F) and severely shortened body axes with compressed somites marked by *myod* expression at 24 hpf (Fig. 8G, H). At 2 dpf these embryos have highly compressed body axes, thick notochords and narrow compressed somites (Fig. 9B; not shown). Like in *col* mutants, we also observe clustering of melanophores posterior to the otocysts (Fig. 9B). We also observed the ectopic positioning of the hindbrain facial branchiomotor neurons in r4 due to lack of caudal migration as seen in *col* mutants (Fig. 9F). These embryos additionally showed a severe reduction in *islet-1* expression in these neuronal populations (Fig. 9F) as well as a drastic reduction in *dlx2* expression in the forebrain (Fig. 9D). Exposing embryos to higher concentrations of TSA at 5 hpf resulted in high mortality by 24 hpf. In order to determine the effect of blocking HDAC activity later in development, we continuously exposed wildtype embryos to TSA beginning at 16 hpf (Table 6). Embryos at this stage required a higher concentration of TSA (800 nM) to show phenotypes resembling *col* mutants. These embryos partially phenocopied the *col* mutant phenotype. Treated embryos at 2 dpf developed stunted body axes, the melanophore migration defect and had pectoral fins (Fig. 9A; not shown). These

embryos also displayed aberrant branchiomotor hindbrain neuronal migration (Fig. 9E). In contrast to untreated *col* mutant embryos, *dlx2* expression in the forebrain is only slightly reduced in treated wildtype embryos (Fig. 9C) compared to untreated wildtype embryos. Early notochord development also appeared unaffected in treated embryos (not shown). Treatment of wildtype embryos with 1200nM TSA resulted in widespread cell death in treated embryos by 2 dpf. Together, these results suggest an early requirement for HDAC function in brain patterning and notochord development whereas extension of the body axis, tangential migration of hindbrain facial branchiomotor neurons, pectoral fin development and melanophore patterning, require or also require HDAC function at relatively later stages of development.

Discussion

We have previously shown that the zebrafish mutant *col* displays specific defects in early DV patterning and AP patterning of the neuroectoderm (Nambiar and Henion, 2004). Our results indicated a function for Col as an inhibitor of canonical Wnt signaling (Nambiar and Henion, 2004). Our data also showed that while the early DV patterning and the neural AP patterning defects in *col* mutants were rescued by blocking excessive canonical Wnt signaling, these embryos still retained compressed body axes and notochords. Blocking of *wnt8* function using *wnt8* MOs was able to partially rescue body curvature (Nambiar and Henion, 2004) and this may be attributed to the activation of molecules such as Stat3 that are activated by the canonical Wnt pathway and regulate the initiation of CE (Sepich et al., 2005). These embryos, however, still are distinctly shorter than wildtype siblings.

In this study, we detail the defects in the extension of the body axis and notochord as well as the caudal migration of hindbrain nVII branchiomotor neurons in *col* mutants. We have identified *col* as zebrafish *histone deacetylase 1*. Our results indicate novel functions for *col/hdac1* in non-canonical Wnt/PCP signaling during axial extension and in Wnt-indpendent hindbrain branchiomotor neuronal migration.

col encodes the *histone deacetylase 1* gene

The *hdac1* gene in *col* ^{b382}mutants harbors a T to G tranversion in the intron flanking exon 5. This creates a new splice acceptor site resulting in the insertion of three additional amino acids in one of seven highly conserved motifs in the Hdac1 protein. Misexpression of *hdac1* mRNA in *col*$^{-/-}$ embryos rescues all aspects of the mutant phenotype and morpholino-mediated knockdown of the gene in wildtype embryos phenocopies *col* mutants. *col* mutant embryos very closely resemble other *hdac1* mutants such as *add* and *t24411* (Yamaguchi et al., 2005; Stadler et al., 2005), and correctly spliced *hdac1* transcripts appear to be absent in *col* mutants, consistent with the possibility that *col* ^{b382} locus may correspond to a null mutation of *hdac1*. However, we cannot rule out partial functionality of Col mutant protein or the presence of wildtype *hdac1* transcripts in *col* mutants at levels below the detection limits of the methods we used. Thus, we cannot at present conclude that *col* represents a null *hdac1* mutation (and see below).

Histone deacetylases play an important role in maintaining equilibrium between the acetylated and deacetylated states of chromatin and thus the tissue-specific expression status of genes and can also play a critical role in regulating the extracellular microenvironment (Whetstine et al., 2005). In zebrafish, *hdac1* has been shown to regulate cell cycle exit and subsequent neurogenesis in the retina (Stadler et al., 2005; Yamaguchi et al., 2005) by antagonizing both the Notch and canonical Wnt signaling pathways (Yamaguchi et al., 2005). In addition to this, data from Cunliffe (2004) implicates *hdac1* in promoting neuronal specification in the developing zebrafish brain by repressing Notch target gene expression. Our data provides the first evidence, in either vertebrates or invertebrates, for the functioning of *hdac1* in regulating

body extension and neuronal migration in the early embryo. Further, we show that *hdac1* is involved in the regulation of these processes by means of the non-canonical Wnt/PCP pathway as well as independent of this pathway but involving genetic interaction with *vangl2*, respectively.

The role of Hdac1 in the non-canonical Wnt/PCP pathway

col mutants exhibit phenotypes characteristic of reduced non-canonical Wnt/PCP pathway signaling. By 2 dpf these mutant embryos typically develop stunted body axes, thick, short notochords and rounded somites. Similar phenotypes are observed in *slb/wnt11* (Heisenberg et al., 2000), *ppt/wnt5a* (Rauch et al., 1997), *tri/vangl2* (Sepich et al., 2000), *kny/glp4* (Topczewski et al., 2001) mutants and *pk* morphants (Carreira-Barbosa et al., 2003). Consistent with this, activating the non-canonical pathway by overexpressing Δ*Ndsh* (Heisenberg et al., 2000), *rho kinase2* and *vangl2* is able to completely rescue extension of the body axis and notochord and somite defects in *col* mutants. Our results, therefore, strongly suggest that *col/hdac1* acts as a positive regulator of the non-canonical Wnt/PCP pathway. In contrast, analysis of the actin cytoskeleton of wildtype and *col* mutants during gastrulation revealed no discernable differences between *col* and wildtype embryos. This result is not consistent with compromised *col/hdac1* function disrupting the cellular cytoskeleton generally and indirectly affecting cell polarity. However, it is important to note that this analysis of the cytoskeleton was not comprehensive and we cannot rule out subtle changes. It will be of considerable interest to examine potential defects in the subcellular localization of PCP pathway components during gastrulation in *col* mutants when reagents become available.

A major difference in the phenotypes displayed by other zebrafish Wnt/PCP mutants and *col* is that we do not observe an early manifestation of CE defects in *col* mutant embryos. Other Wnt/PCP mutants display defects in dorsal convergence and extension of the body axis starting at 9 hpf (Heisenberg et al., 2000; Rauch et al., 1997; Sepich et al., 2000; Carreira-Barbosa et al., 2003). In contrast, extension defects in *col* mutants become prominent only by 30 hpf. We have previously reported a similar late development of other mutant phenotypes in *col* such as defects in forebrain and midbrain patterning (Nambiar and Henion, 2004). Given the importance of Hdac1 as a co-repressor in yeast and mammalian systems, *col* mutants might be expected to display more severe patterning defects. It is possible that the persistence of maternal histone deacetylase and the activity of other Hdacs in *col* mutants may account for the lack of severe early CE defects in *col* mutants. Supporting this, we have shown that treating wildtype embryos with TSA, a potent inhibitor of all Hdacs, at different developmental time points results in different phenotypes. Early TSA treatment (5 hpf) produces embryos with CE defects similar to those observed in other zebrafish Wnt/PCP mutants and more severe than *col* mutants. Later treatment of embryos with TSA (16 hpf) produced embryos with milder defects that closely resembled *col* mutants. Since embryos exposed to TSA starting at the later time point displayed defects in extension of the body axis we suggest that persistent HDAC activity is required for extension movements during the later stages of development. Similar to *col*, *Drosophila* null mutants for *rpd3*, the *hdac1* homolog, also display mild embryonic defects that have been attributed to possible redundancy among *Drosophila* histone deacetylases (Mannervik and Levine, 1999). Interestingly, *Hdac1*-null mouse ES cells show a marked compensatory increase in *Hdac2* and *Hdac3* expression (Lagger et al., 2002), lending further support to the possibility that functional redundancy among Hdacs and/or different maternal and zygotic functional contributions account for the phenotypes of *col* and other zebrafish *hdac1* mutants. Nevertheless, we do observe an early DV patterning defect in *col* mutants attributable to disregulation of canonical Wnt signaling (Nambiar and Henion, 2004), which although not severe, suggests that neither maternal *hdac1* function or the activities of other histone deacetylases can completely compensate for a requirement for early embryonic zygotic *hdac1* function.

col/hdac1 is involved in mediating tangential migration of hindbrain facial (nVII) branchiomotor neurons

A number of genes that are required for both CE and neuronal migration have been identified so far. Amongst them are *tri/vangl2* (Bingham et al., 2002; Jessen et al., 2002), *pk1* (Carreira-Barbosa et al., 2003) and *llk/scrb1* (Wada et al., 2005). Other signaling molecules in the non-canonical Wnt pathway such as *slb/wnt11, ppt/wnt5a* and *kny/glypican4/6* regulate CE movements in the gastrula (Topczewski et al., 2001; Heisenberg et al., 2000; Kilian et al., 2003), but do not regulate neuronal migration (Bingham et al., 2002; Jessen et al., 2002). Also, branchiomotor neuronal migration is unaffected by the overexpression of a dominant negative form of Dsh which is able to suppress Wnt/PCP-mediated CE movements (Bingham et al., 2002; Jessen et al., 2002). These results therefore support the hypothesis that *vangl2, pk1* and *scrb1* regulate neuronal migration via a pathway independent of the Wnt/PCP signaling cascade.

In this study, we have shown that *col* mutants, in addition to extension defects, display aberrant migration of facial (nVII) hindbrain branchiomotor neurons. These neurons are born in the correct positions in the rhombomere 4 (Higashijima et al., 2000), but while their wildtype counterparts migrate caudally into rhombomeres 6 and 7 (Chandrasekhar et al., 1997), these neurons persist in their original positions. We were unable to test if these neurons function in their ectopic positions because of embryonic lethality. However, in a previous study it has been shown that these ectopic neurons in *hdac1*$^{-/-}$ mutants form axonal projections (Cunliffe, 2004).

Our studies also reveal that this migration defect is not a result of a more general effect of *hdac1* on hindbrain patterning. Rhombomere formation and the development of the patterning of other hindbrain neurons are unaffected in *col*. Previous studies by Cunliffe (2004) also revealed no defects in segmentation of the hindbrain of *hdac1* mutant embryos although he did report perturbed segmental organization of hindbrain Hu-expressing neurons. We, however, did not observe any defects in the organization of two sets of neurons arranged segmentally in the hindbrain of *col* mutants - the reticulospinal neurons and the commissural neurons. We did observe a decrease in the number of these neurons that is consistent with fewer Hu-positive hindbrain neurons reported by Cunliffe in *hdac1* mutants suggesting that *hdac1* function is required for the specification of neurons in the hindbrain. Consistent with results published by Cunliffe we also observed fewer cell bodies in the neuronal cluster marked by islet-1 antibody making them very difficult to detect. The intensity of the signal in situ preparations from mutant and wild-type however were not considerably different.

We were able to restore normal migration of these neurons by overexpressing *vangl2/tri*. Consistent with previous data, other components of the Wnt/PCP pathway such as Δ*Ndsh* and *rhokinase2* were unable to rescue the neuronal migration defect. This suggests that this phenotype is not a consequence of the CE defects observed in *col* and raises the possibility that Hdac1 functions along with Vangl2 via an independent pathway to regulate the migration of these neurons. These defects in neuronal migration are also not a consequence of aberrant canonical Wnt signaling since overexpression of negative regulators of the canonical Wnt pathway are not able to restore normal migration of the r4 neurons (not shown). We also found that defects in general patterning of the hindbrain do not contribute to the aberrant migration of these neurons since the expression patterns of segmentally expressed genes *krox20, val* and *hoxb3* and the patterning of other hindbrain neuronal populations such as the reticulo-spinal neurons and commissural neurons are normal.

We were also able to phenocopy this defect with injection of *hdac1* MOs and treatment with TSA. Embryos treated with TSA during early development, in addition to defects in the migration of branchiomotor neurons, also displayed a reduction in the *islet-1* expression in

these neurons. Previous data from Cunliffe (2004) has implicated *hdac1* in the specification of hindbrain branchiomotor neurons, raising the possibility that the reduction in *islet-1* expression in these TSA treated embryos could be due to defects in specification of this subset of neurons. We also show that treatment of wildtype embryos with TSA during later stages (at 21 hpf and 24 hpf; not shown) resulted in aberrant neuronal migration suggesting that continued Hdac activity is required for caudal migration of the facial branchiomotor neurons.

Novel functions of Hdac1 in the Wnt/PCP pathway

Our studies of *col* mutants have revealed novel functions of Hdac1 in major signaling pathways regulating embryonic development. However, precisely how Hdac1 functions in these pathways is not fully understood. In the canonical Wnt pathway (see Nambiar and Henion, 2004), Hdac1 functions as a co-repressor with molecules such as Groucho and LEF1 in the nucleus (Brantjes et al., 2001; Chen et al., 1999; Billin et al., 2000). Studies in *Drosophila* and vertebrates have shown that Groucho, a canonical Wnt signaling pathway repressor, readily interacts with Hdac1 forming a repressor complex that remains tethered to the promoter of Wnt target genes (Brantjes et al., 2001; Chen et al., 1999). Data also indicates that the Wnt transcription factor LEF1 can act as a repressor in the presence of Hdac1 (Billin et al., 2000). Activation of LEF-dependent target genes occurs when the increasing level of β-catenin in the nucleus is able to dissociate Hdac1 from LEF1 and itself bind to LEF1 to form a dimeric activator (Billin et al., 2000). Thus, Hdac1 appears to maintain Wnt target genes in a repressed state until replaced by activators such as β-catenin (Billin et al., 2000).

In this study we have shown that *col/hdac1* regulates both the non-canonical Wnt/PCP pathway that controls CE movements as well as the pathway that mediates the caudal migration of hindbrain facial motor neurons. There are a number of possible ways in which Hdac1 functions in these pathways. For example, since Hdac1 regulates both pathways, it is conceivable then that Col/Hdac1 could act by regulating the transcription of *vangl2* or its interacting proteins. We examined *vangl2* expression in *col* mutants and there appeared to be no significant difference compared to wildtype siblings (not shown). Another possible scenario for the functioning of Col/Hdac1 in this context could be via an interaction with Vangl2 and its interacting proteins such as Pk and Scribble that act at the common branchpoint. Another possibility is that Col/Hdac1 regulates the transcription of other components of the Wnt/PCP pathway and/or the targets of Wnt/PCP pathway genes. In the latter case, additional interactions of Hdac1 with Wnt/PCP signaling-independent genes or components of the pathway that also regulate branchiomotor neuron migration are possible. Further studies exploring the function of *col* should reveal the molecular mechanism by which *col/hdac1* affects the activities of the genes involved in the morphogenetic events we have described.

Supplementary Material

Refer to Web version on PubMed Central for supplementary material.

Acknowledgments

We thank our colleagues for providing numerous reagents and are particularly thankful to Will Talbot. This work was supported by NSF grant IBN0315765 with additional support from NIH grant P30-NS045758.

References

Adler PN, Lee H. Frizzled signaling and cell-cell interactions in planar polarity. Curr Opin Cell Biol 2001;13:635–640. [PubMed: 11544034]

Akimenko MA, Ekker M, Wegner J, Lin W, Westerfield M. Combinatorial expression of three zebrafish genes related to *distal-less*: part of a homeobox gene code for the head. J Neurosci 1994;14:3475–86. [PubMed: 7911517]

Allfrey VG. Structural modifications of histones and their possible role in the regulation of ribonucleic acid synthesis. Proc Can Cancer Conf 1966;6:313–35.

Billin AN, Thirlwell H, Ayer DE. Beta-catenin-histone deacetylase interactions regulate the transition of LEF1 from a transcriptional repressor to an activator. Mol Cell Biol 2000;20:6882–90. [PubMed: 10958684]

Bingham S, Higashijima S, Okamoto H, Chandrasekhar A. The Zebrafish *trilobite* gene is essential for tangential migration of branchiomotor neurons. Dev Biol 2002;242:149–60. [PubMed: 11820812]

Boutros M, Mlodzik M. Dishevelled: at the crossroads of divergent intracellular signaling pathways. Mech Dev 1999;83:27–37. [PubMed: 10507837]

Brantjes H, Roose J, van De Wetering M, Clevers H. All Tcf HMG box transcription factors interact with Groucho-related co-repressors. Nucleic Acids Res 2001;29:1410–9. [PubMed: 11266540]

Carreira-Barbosa F, Concha ML, Takeuchi M, Ueno N, Wilson SW, Tada M. Prickle 1 regulates cell movements during gastrulation and neuronal migration in zebrafish. Development 2003;130:4037–46. [PubMed: 12874125]

Chandrasekhar A, Moens CB, Warren JT Jr, Kimmel CB, Kuwada JY. Development of branchiomotor neurons in zebrafish. Development 1997;124:2633–44. [PubMed: 9217005]

Chen G, Fernandez J, Mische S, Courey AJ. A functional interaction between the histone deacetylase Rpd3 and the corepressor groucho in Drosophila development. Genes Dev 1999;13:2218–30. [PubMed: 10485845]

Cunliffe VT. Histone deacetylase 1 is required to repress Notch target gene expression during zebrafish neurogenesis and to maintain the production of motoneurones in response to hedgehog signalling. Development 2004;131:2983–95. [PubMed: 15169759]

de Ruijter AJ, van Gennip AH, Caron HN, Kemp S, van Kuilenburg AB. Histone deacetylases (HDACs): characterization of the classical HDAC family. Biochem J 2003;370:737–49. [PubMed: 12429021]

Dominguez I, Mizuno J, Wu H, Song DH, Symes K, Seldin DC. Protein kinase CK2 is required for dorsal axis formation in Xenopus embryos. Dev Biol 2004;274:110–24. [PubMed: 15355792]

Hammerschmidt M, Pelegri F, Mullins MC, Kane DA, Brand M, van Eeden FJ, Furutani-Seiki M, Granato M, Haffter P, Heisenberg CP, Jiang YJ, Kelsh RN, Odenthal J, Warga RM, Nusslein-Volhard C. Mutations affecting morphogenesis during gastrulation and tail formation in the zebrafish, Danio rerio. Development 1996;123:143–51. [PubMed: 9007236]

Heisenberg CP, Tada M, Rauch GJ, Saude L, Concha ML, Geisler R, Stemple DL, Smith JC, Wilson SW. Silberblick/Wnt11 mediates convergent extension movements during zebrafish gastrulation. Nature 2000;405:76–81. [PubMed: 10811221]

Henion PD, Raible DW, Beattie CE, Stoesser KL, Weston JA, Eisen JS. Screen for mutations affecting development of Zebrafish neural crest. Dev Genet 1996;18:11–7. [PubMed: 8742830]

Higashijima S, Hotta Y, Okamoto H. Visualization of cranial motor neurons in live transgenic zebrafish expressing green fluorescent protein under the control of the *islet-1* promoter/enhancer. J Neurosci 2000;20:206–18. [PubMed: 10627598]

Jenuwein T, Allis CD. Translating the histone code. Science 2001;293:1074– 80. [PubMed: 11498575]

Jessen JR, Topczewski J, Bingham S, Sepich DS, Marlow F, Chandrasekhar A, Solnica-Krezel L. Zebrafish *trilobite* identifies new roles for Van gogh-like protein 2 in gastrulation and neuronal movements. Nat Cell Biol 2002;4:610–5. [PubMed: 12105418]

Kane DA, Warga RM. Domains of movement in the zebrafish gastrula. Semin Dev Biol 1994;5:101–109.

Kelly GM, Greenstein P, Erezyilmaz DF, Moon RT. Zebrafish *wnt8* and *wnt8b* share a common activity but are involved in distinct developmental pathways. Development 1995;121:1787–99. [PubMed: 7600994]

Kibar Z, Vogan KJ, Groulx N, Justice MJ, Underhill DA, Gros P. Ltap, a mammalian homolog of Drosophila Van gogh-like protein 2/Van Gogh, is altered in the mouse neural tube mutant Loop-tail. Nat Genet 2001;28:251–5. [PubMed: 11431695]

Kilian B, Mansukoski H, Barbosa FC, Ulrich F, Tada M, Heisenberg CP. The role of Ppt/Wnt5 in regulating cell shape and movement during zebrafish gastrulation. Mech Dev 2003;120:467–76. [PubMed: 12676324]

Kim CH, Ueshima E, Muraoka O, Tanaka H, Yeo SY, Huh TL, Miki N. Zebrafish *elav*/HuC homologue as a very early neuronal marker. Neurosci Lett 1996;216:109–12. [PubMed: 8904795]

Knapik EW, Goodman A, Atkinson OS, Roberts CT, Shiozawa M, Sim CU, Weksler-Zangen S, Trolliet MR, Futrell C, Innes BA, Koike G, McLaughlin MG, Pierre L, Simon JS, Vilallonga E, Roy M, Chiang PW, Fishman MC, Driever W, Jacob HJ. A reference cross DNA panel for zebrafish (Danio rerio) anchored with simple sequence length polymorphisms. Development 1996;123:451–60. [PubMed: 9007262]

Korzh V, Edlund T, Thor S. Zebrafish primary neurons initiate expression of the LIM homeodomain protein Isl-1 at the end of gastrulation. Development 1993;118:417–25. [PubMed: 8223269]

Marks PA, Miller T, Richon VM. Histone deacetylases. Curr Opin Pharmacol 2003;3:344–51. [PubMed: 12901942]

Marlow F, Topczewski J, Sepich D, Solnica-Krezel L. Zebrafish Rho kinase 2 acts downstream of Wnt11 to mediate cell polarity and effective convergence and extension movements. Curr Biol 2002;11:876–84. [PubMed: 12062050]

McKay RM, Peters JM, Graff JM. The casein kinase I family in Wnt signaling. Dev Biol 2001;235:388–96. [PubMed: 11437445]

Moens CB, Yan YL, Appel B, Force AG, Kimmel CB. *valentino*: a zebrafish gene required for normal hindbrain segmentation. Development 1996;122:3981–90. [PubMed: 9012518]

Myers DC, Sepich DS, Solnica-Krezel L. Convergence and extension in vertebrate gastrulae: cell movements according to or in search of identity? Trends Genet 2002;18:447–55. [PubMed: 12175805]

Nambiar RM, Henion PD. Sequential antagonism of early and late Wnt-signaling by zebrafish *colgate* promotes dorsal and anterior fates. Dev Biol 2004;267:165–80. [PubMed: 14975724]

Odenthal J, Nusslein-Volhard C. *fork head* domain genes in zebrafish. Dev Genes Evol 1998;208:245–58. [PubMed: 9683740]

Park M, Moon RT. The planar cell polarity gene *vangl2* regulates cell behavior and cell fate in vertebrate embryos. Nat Cell Biol 2002;4:20–25. [PubMed: 11780127]

Prince VE, Moens CB, Kimmel CB, Ho RK. Zebrafish hox genes: expression in the hindbrain region of wild-type and mutants of the segmentation gene, valentino. Development 1998;125:393–406. [PubMed: 9425135]

Rauch GJ, Hammerschmidt M, Blader P, Schauerte HE, Strahle U, Ingham PW, McMahon AP, Haffter P. Wnt5 is required for tail formation in the zebrafish embryo. Cold Spring Harb Symp Quant Biol 1997;62:227–34. [PubMed: 9598355]

Rice JC, Allis CD. Code of silence. Nature 2001;414:258–61. [PubMed: 11713509]

Schulte-Merker S, Ho RK, Herrmann BG, Nusslein-Volhard C. The protein product of the zebrafish homologue of the mouse T gene is expressed in nuclei of the germ ring and the notochord of the early embryo. Development 1992;116:1021–32. [PubMed: 1295726]

Schwarz-Romond T, Asbrand C, Bakkers J, Kuhl M, Schaeffer HJ, Huelsken J, Behrens J, Hammerschmidt M, Birchmeier W. The ankyrin repeat protein Diversin recruits Casein kinase Iepsilon to the beta-catenin degradation complex and acts in both canonical Wnt and Wnt/JNK signaling. Genes Dev 2002;16:2073–84. [PubMed: 12183362]

Sepich DS, Calmelet C, Kiskowski M, Solnica-Krezel L. Initiation of convergence and extension movements of lateral mesoderm during zebrafish gastrulation. Dev Dyn 2005;234:279–92. [PubMed: 16127722]

Sepich DS, Myers DC, Short R, Topczewski J, Marlow F, Solnica-Krezel L. Role of the zebrafish *trilobite* locus in gastrulation movements of convergence and extension. Genesis 2000;27:159–73. [PubMed: 10992326]

Shulman JM, Perrimon N, Axelrod JD. Frizzled signaling and the developmental control of cell polarity. Trends Genet 1998;14:452–8. [PubMed: 9825673]

Simons M, Gloy J, Ganner A, Bullerkotte A, Bashkurov M, Kronig C, Schermer B, Benzing T, Cabello OA, Jenny A, Mlodzik M, Polok B, Driever W, Obara T, Walz G. Inversin, the gene product mutated

in nephronophthisis type II, functions as a molecular switch between Wnt signaling pathways. Nat Genet 2005;37:537–43. [PubMed: 15852005]

Solnica-Krezel L, Stemple DL, Driever W. Transparent things: cell fates and cell movements during early embryogenesis of zebrafish. Bioessays 1995;17:931–9. [PubMed: 8526887]

Solnica-Krezel L, Stemple DL, Mountcastle-Shah E, Rangini Z, Neuhauss SC, Malicki J, Schier AF, Stainier DY, Zwartkruis F, Abdelilah S, Driever W. Mutations affecting cell fates and cellular rearrangements during gastrulation in zebrafish. Development 1996;123:67–80. [PubMed: 9007230]

Stadler JA, Shkumatava A, Norton WH, Rau MJ, Geisler R, Fischer S, Neumann CJ. Histone deacetylase 1 is required for cell cycle exit and differentiation in the zebrafish retina. Dev Dyn 2005;233:883–9. [PubMed: 15895391]

Strahl BD, Allis CD. The language of covalent histone modifications. Nature 2000;403:41–5. [PubMed: 10638745]

Tada M, Smith JC. Xwnt11 is a target of Xenopus Brachyury regulation of gastrulation movements via Dishevelled, but not through the canonical Wnt pathway. Development 2000;127:2227–38. [PubMed: 10769246]

Topczewski J, Sepich DS, Myers DC, Walker C, Amores A, Lele Z, Hammerschmidt M, Postlethwait J, Solnica-Krezel L. The zebrafish glypican *knypek* controls cell polarity during gastrulation movements of convergent extension. Dev Cell 2001;1:251–64. [PubMed: 11702784]

Trevarrow B, Marks DL, Kimmel CB. Organization of hindbrain segments in the zebrafish embryo. Neuron 1990;4:669–79. [PubMed: 2344406]

Veeman MT, Slusarski DC, Kaykas A, Louie SH, Moon RT. Zebrafish *prickle*, a modulator of noncanonical Wnt/Fz signaling, regulates gastrulation movements. Curr Biol 2003;13:680–5. [PubMed: 12699626]

Wallingford JB, Fraser SE, Harland RM. Convergent extension: the molecular control of polarized cell movement during embryonic development. Dev Cell 2002;2:695–706. [PubMed: 12062082]

Weinberg ES, Allende ML, Kelly CS, Abdelhamid A, Murakami T, Andermann P, Doerre OG, Grunwald DJ, Riggleman B. Developmental regulation of zebrafish MyoD in wild-type, *no tail* and *spadetail* embryos. Development 1996;122:271–80. [PubMed: 8565839]

Whetstine JR, Ceron J, Ladd B, Dufourcq P, Reinke V, Shi Y. Regulation of tissue-specific and extracellular matrix-related genes by a class I histone deacetylase. Mol Cell 2005;18:483–90. [PubMed: 15893731]

Wilkinson DG, Bhatt S, Chavrier P, Bravo R, Charnay P. Segment-specific expression of a zinc-finger gene in the developing nervous system of the mouse. Nature 1989;337:461–4. [PubMed: 2915691]

Willert K, Brink M, Wodarz A, Varmus H, Nusse R. Casein kinase 2 associates with and phosphorylates *dishevelled*. EMBO J 1997;16:3089–96. [PubMed: 9214626]

Yamaguchi M, Tonou-Fujimori N, Komori A, Maeda R, Nojima Y, Li H, Okamoto H, Masai I. Histone deacetylase 1 regulates retinal neurogenesis in zebrafish by suppressing Wnt and Notch signaling pathways. Development 2005;132:3027–43. [PubMed: 15944187]

Yan D, Wallingford JB, Sun TQ, Nelson AM, Sakanaka C, Reinhard C, Harland RM, Fantl WJ, Williams LT. Cell autonomous regulation of multiple Dishevelled-dependent pathways by mammalian Nkd. Proc Natl Acad Sci USA 2001;98:3802–7. [PubMed: 11274398]

Yoshida M, Horinouchi S, Beppu T. Trichostatin A and trapoxin: novel chemical probes for the role of histone acetylation in chromatin structure and function. BioEssays 1995;17:423–430. [PubMed: 7786288]

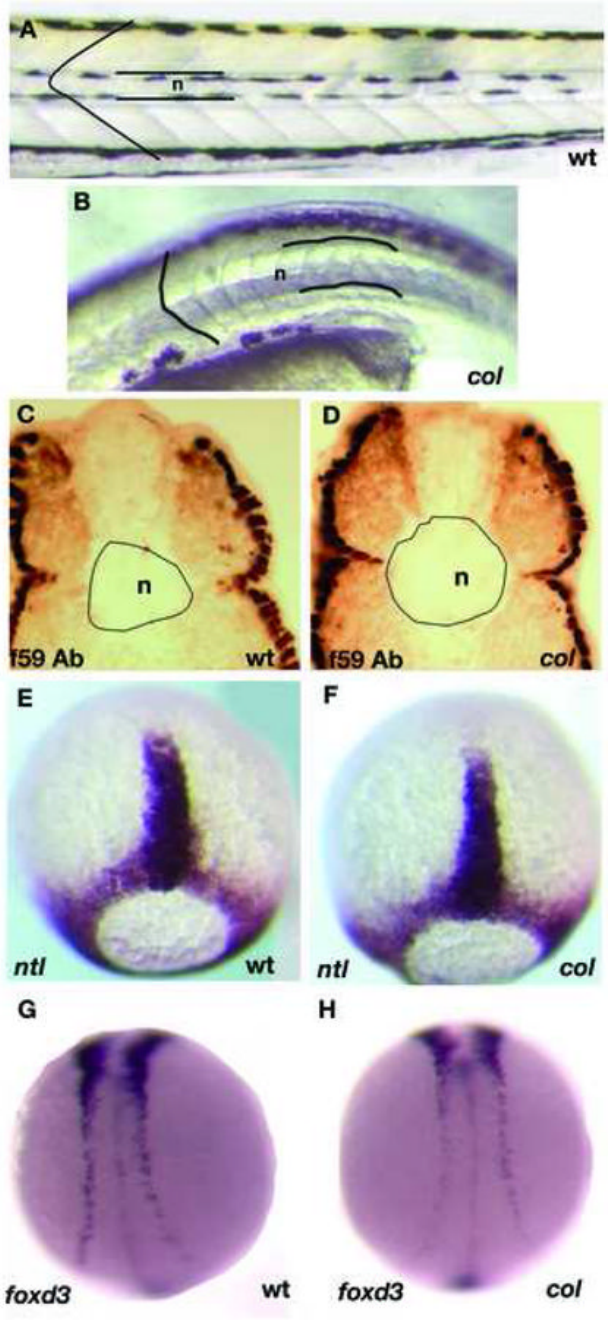

Figure 1. *col*mutant embryos display a late axial extension phenotype

Live *col* mutants at 4 dpf (B) have wider notochords (n) than their wildtype siblings (A). Larger notochord diameter is observed in cross-sections of the trunk of 2 dpf *col* mutants stained with antibody f59 (D) as compared to wildtype (C). *col* mutants also display rounded somite morphology (B) unlike chevron-shaped wildtype somites (A). In contrast, *col* mutants do not display prominent early CE defects. For example, *ntl* expression in the notochord anlage at late gastrulation of *col* embryos (F) is indistinguishable from wildtype embryos (E). The degree of convergence of the neural plate border at the 12-somite stage identified by *foxd3* expression also appears normal in *col* mutants (C, D).

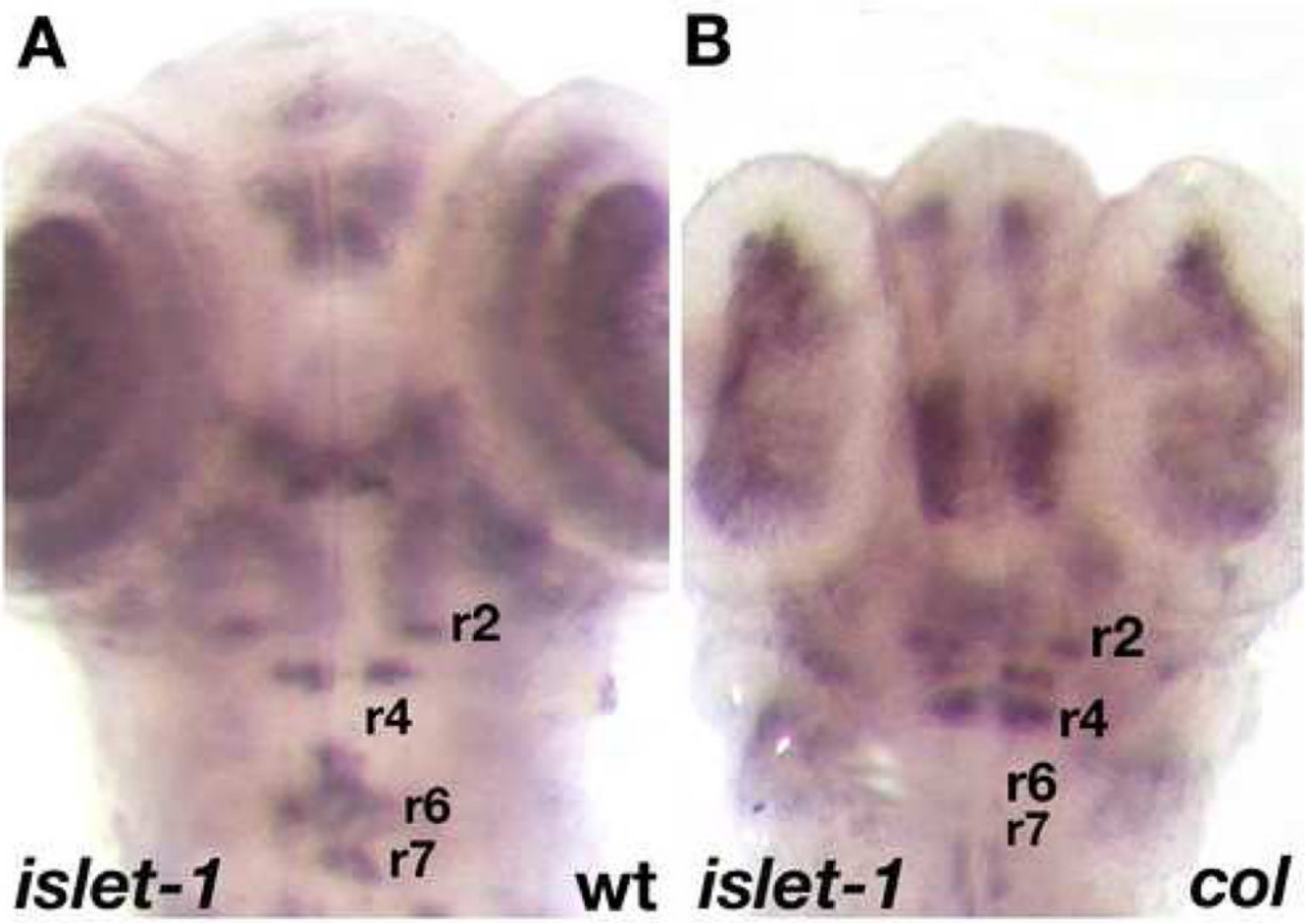

Figure 2. Facial (nVII) hindbrain neurons in *col* mutants do not migrate tangentially

Hindbrain neurons are marked by *islet1* expression (A, B) at 56 hpf. In *col* mutant,, nVII neurons fail to migrate into r6 and r7 (B) as in wildtype siblings (A). In contrast, nV neurons are positioned correctly in mutants.

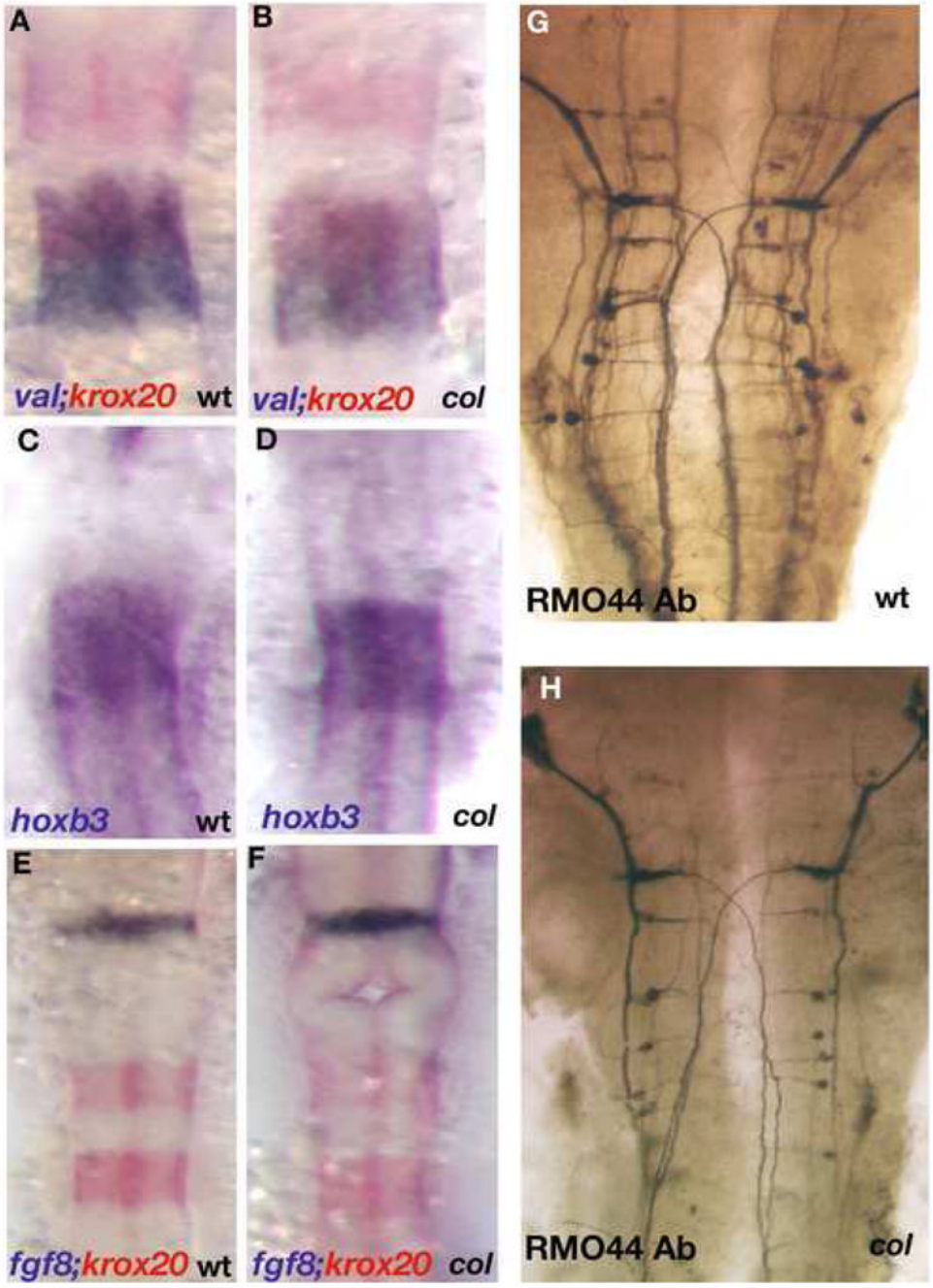

Figure 3. Gross patterning of the hindbrain is unperturbed in *col* mutants

Hindbrain rhombomere patterning appears undisturbed in *col* mutant embryos (B, D, F) as compared to wild-type (A, C, E). *Krox20* (red) labels r3 and r5 and *valentino* (blue) marks r5 and r6 (A, B). *hoxb3* also marks r5 and r6 (C, D). *fgf8* (blue) labels the mid-hindbrain boundary and *krox20* (red) marks r3 and r5 showing that gross development between the mid-hindbrain boundary and r3 in the hindbrain also appears normal in *col* mutant embryos (F as compared to E). RMO44 labels reticulospinal neurons (G, H). The patterning of this neuronal population is relatively unperturbed in *col* mutants although overall neuronal numbers appear to be reduced (see Results).

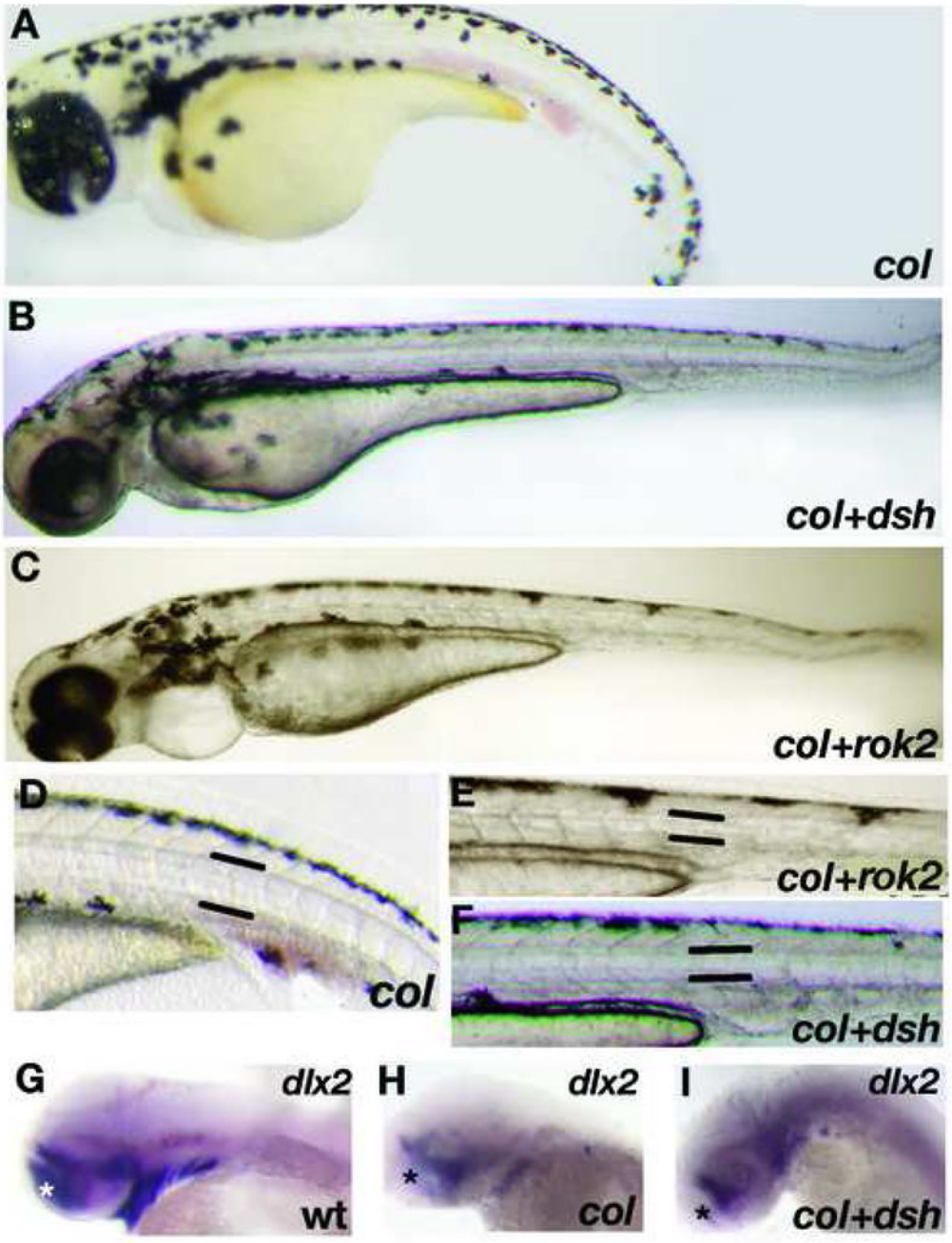

Figure 4. Regulators of the Wnt/PCP pathway are able to partially rescue *col* mutants

Δ*Ndsh* (B, F) and *rok2* (C, E) were able to abolish the short body axis (B, C) and short wide notochords (E, F) observed in *col* mutants at 3 dpf (A, D). However, canonical Wnt signaling regulated defects in *col* mutants still remain in injected embryos. *dlx2* expression in the telencephalon (asterisk) remains reduced compared to wildtype (G) in *rock2* injected *col* mutant embryos (I) as compared to uninjected *col* mutants (H). The persistence of this phenotype is also observed in Δ*Ndsh* injected *col* mutants (not shown).

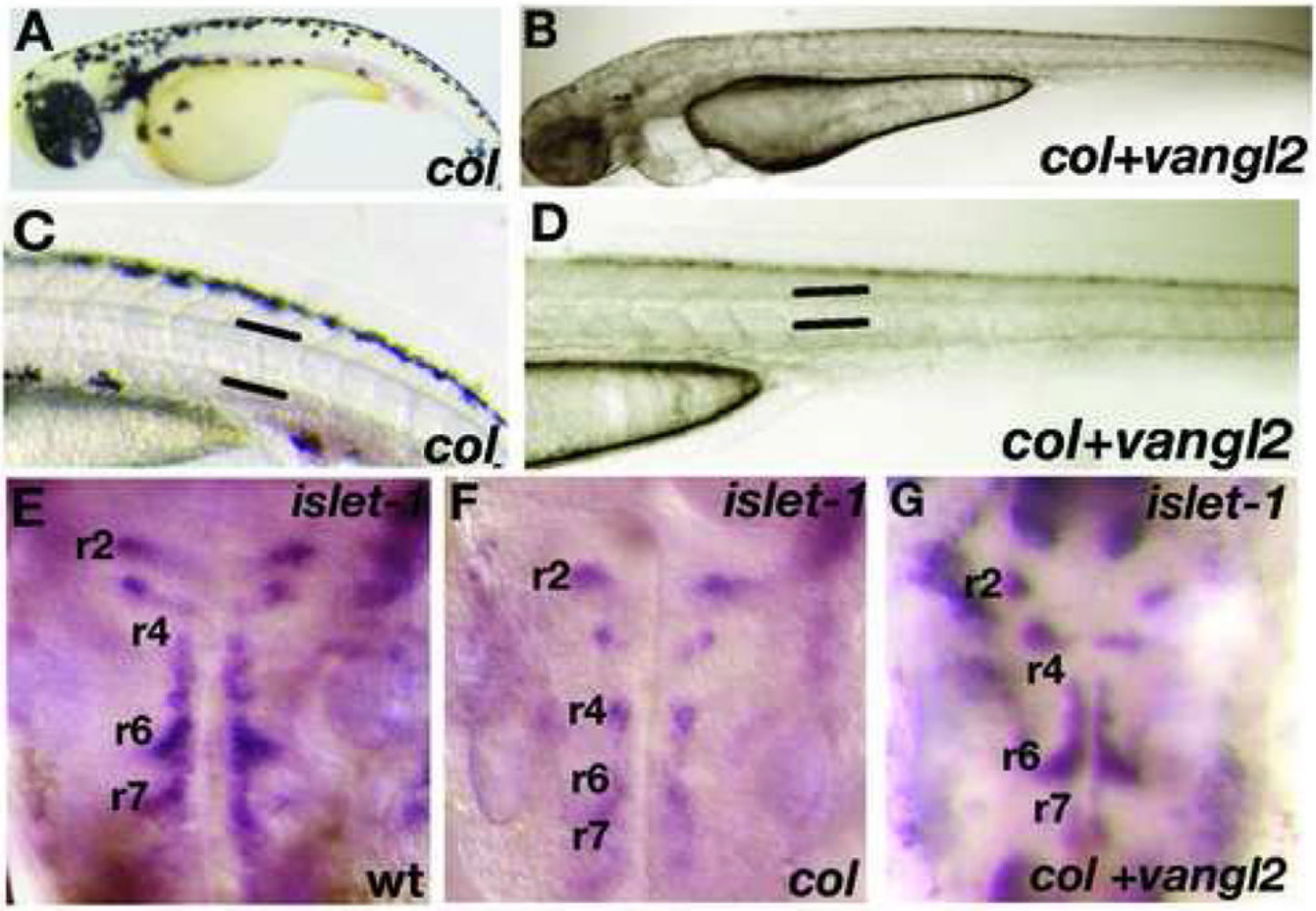

Figure 5. *tri/vangl2*is able to rescue extension defects and tangential migration of hindbrain branchiomotor neurons in *col* mutant embryos

Overexpression of *tri/vangl2* in *col* mutants (B, D) is able to rescue the stunted trunk development and broad notochords observed in uninjected *col* mutants (A, C). Facial (nVII) hindbrain motor neurons labeled by *islet1* expression are positioned ectopically in r4 in *col* mutants at 56 hpf (F) compared to wildtype (E). Overexpression of *tri/vangl2* restores tangential migration of these neurons into r6 and r7 (G) as in wildtype siblings (E). nV neurons are positioned correctly in r2 in *tri/vangl2* injected (G) and uninjected (F) *col* mutants.

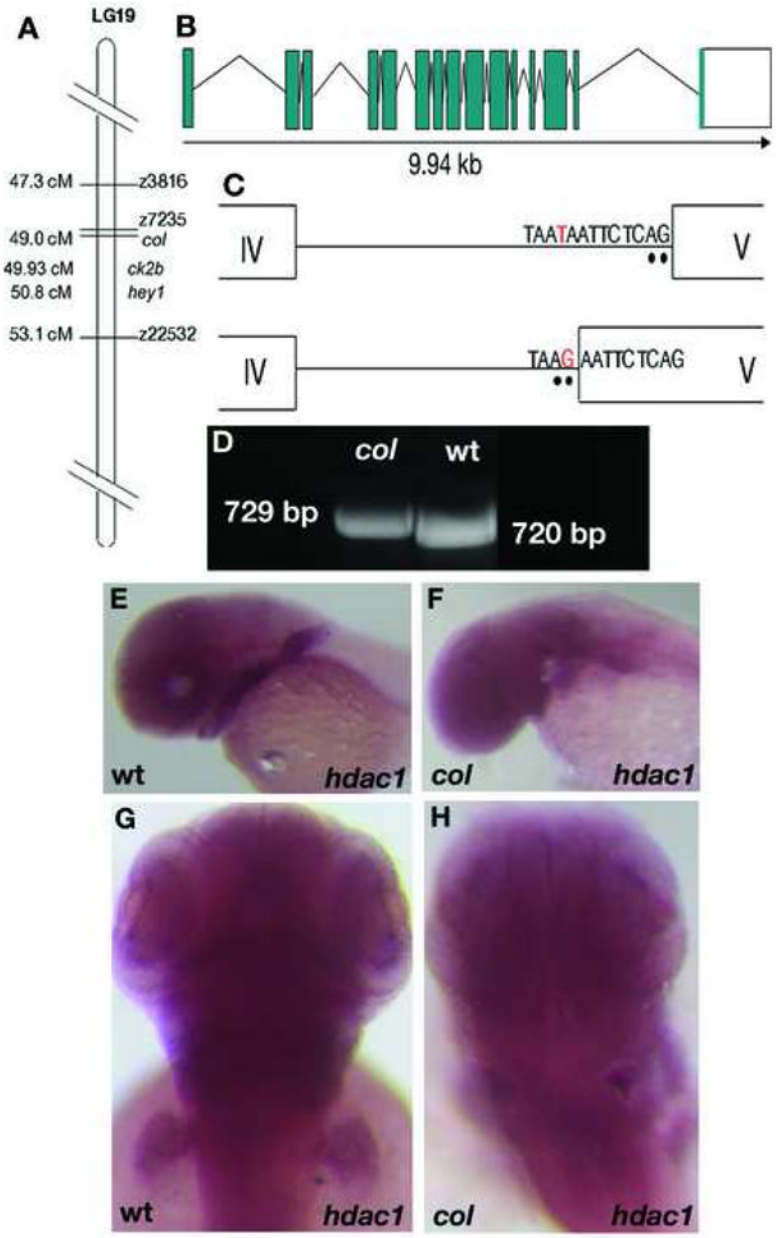

Figure 6. The*col* locus encodes *hdac1*

col maps close to the zebrafish *hdac1* locus on LG 19 (A). A schematic showing the genomic organization of the zebrafish *hdac1* gene (B). The zebrafish *hdac1* gene has 15 exons and 14 introns spanning 9.94 kb of the genome and a T to G transversion in the intronic sequence adjacent to exon 5 causes aberrant splicing between exons 4 and 5 in *col* mutants (C). Aberrantly spliced *hdac1* cDNA fragment in *col* with an additional 9 bp running in lane 1 can be distinguished from the wildtype product running in lane 2 (D). *hdac1* expression is unaffected in 2 dpf *col* mutants (F, H) compared to wildtype (E, G).

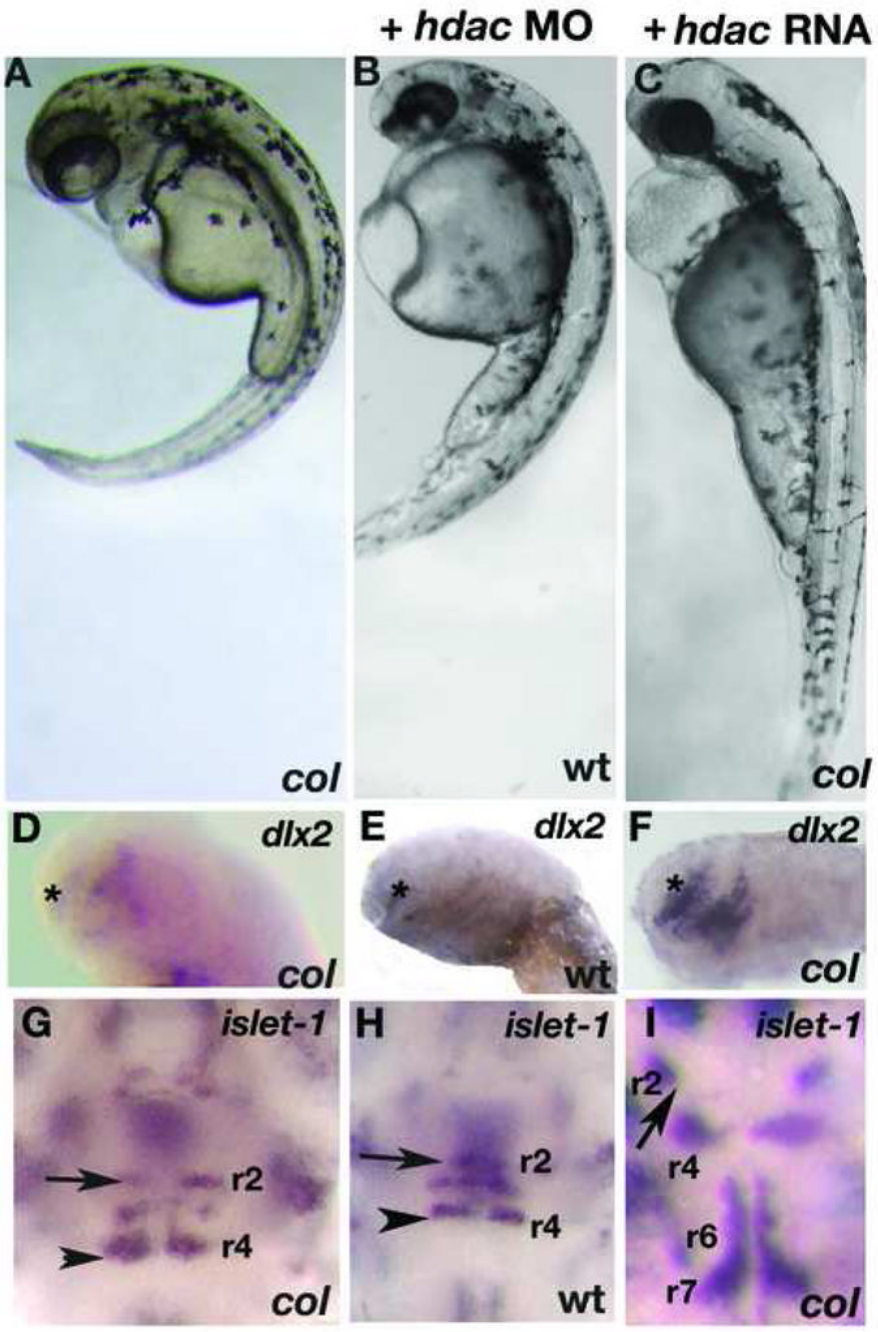

Figure 7. *hdac1* morphants phenocopy *col* mutants and *hdac1* RNA rescues *col* mutant phenotypes

hdac1 MO injected wildtype embryos at 3 dpf (B) resemble uninjected *col* mutants (A). Reduced *dlx2* expression (asterisk) and ectopically positioned facial hindbrain motor neurons (black arrowheads) in *col* mutants (D, G) are phenocopied in *hdac1* morphants (E, H). The position of nV neurons in r2 are marked with arrows (G-I). *hdac1* RNA is able to rescue axis extension and melanophore defects in *col* mutants (C). Telencephalon *dlx2* expression and migration of facial hindbrain motorneurons is restored in *col* mutants injected with *hdac1* RNA (F, I compared to D, G).

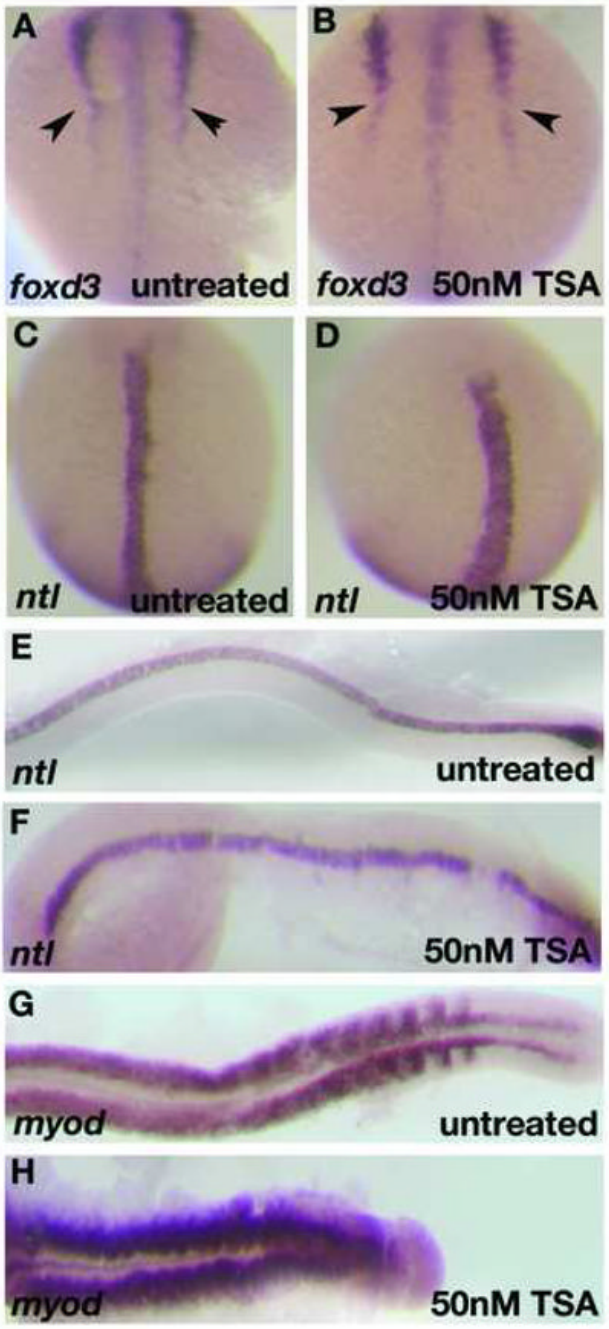

Figure 8. CE defects in early TSA-treated wildtype embryos resembles other zebrafish Wnt/PCP mutants

foxd3 expression at the 6-somite stage in TSA-treated embryos shows defects in convergence (arrowheads; B) as compared to wildtype (A). *ntl* expression at the 6-somite stage (C, D) and 22 hpf (E, F) reveals shorter, thicker notochord in TSA-treated embryos (D, F) than in wildtype embryos (C, E). *myoD* expression at 22 hpf shows compressed, laterally expanded somites in TSA-treated embryos (H) as compared to wildtype (G).

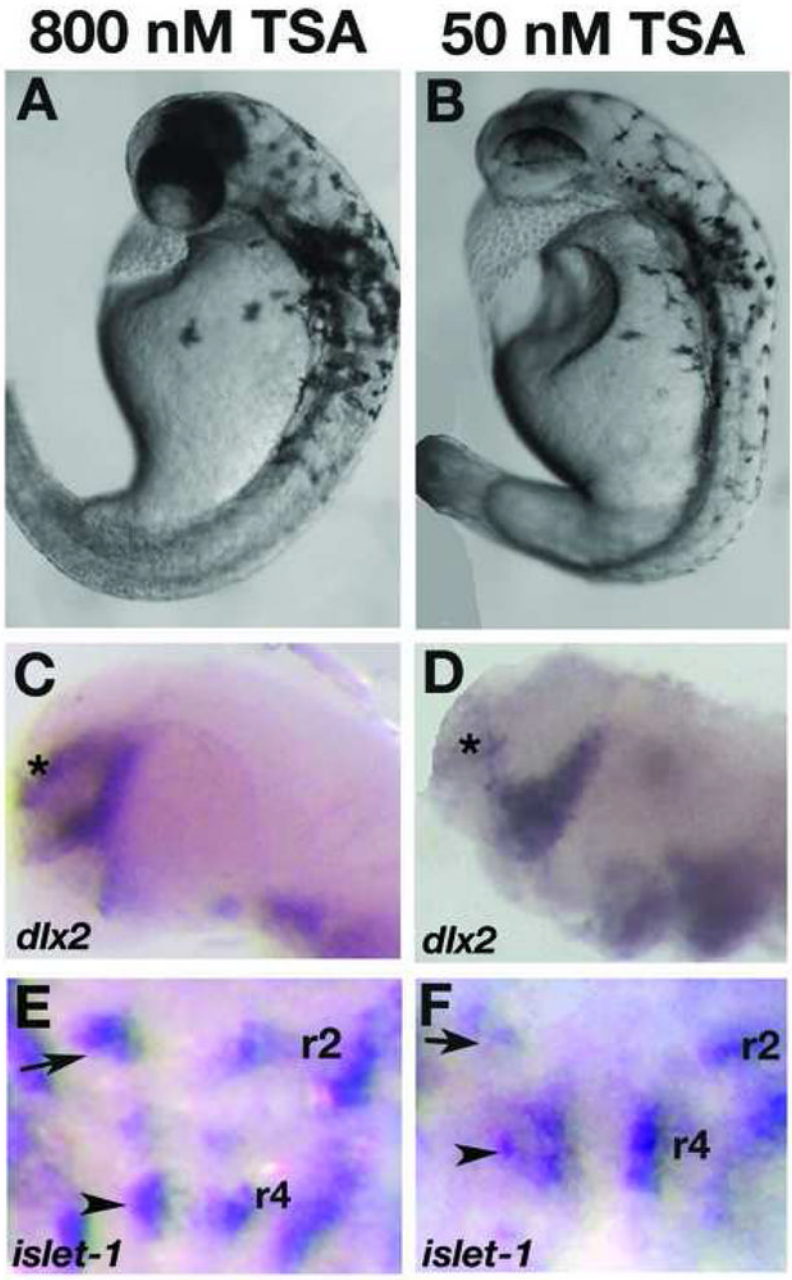

Figure 9. Wildtype embryos treated late with TSA phenocopy *col* mutants

Live wildtype embryos at 2dpf treated with 800 nM TSA late (at 16 hpf) resemble *col* mutants (A, compare to Fig. 7A). *dlx2* expression is unaffected in these embryos (C) while the facial hindbrain motorneurons remain in r4 (arrowhead; E) as in *col* mutants. The position of nV neurons are shown with black arrows. Phenotypes observed at 2dpf in wildtype embryos treated with 50 nM TSA early (5 hpf) appear more severe (B). The forebrain *dlx2* expression domain is reduced (D), similar to *col* mutants, and facial hindbrain motorneurons remain in r4 (F) in these embryos.

Table 1

Statistical analysis of mean length of wild-type and *col/hdac1* embryos at 25 hpf, 48 hpf and 72 hpf.

Hours post fertilization	Mean length of embryos in mm ± 1 SD		P value
	wild-type	*col/hdac1*	
25	2.115± 0.085 n=20	1.943± 0.058 n=20	P< 0.001
48	2.934± 0.054 n=10	2.710± 0.052 n=10	P< 0.001
72	3.466± 0.067 n=10	2.684± 0.184 n=10	P< 0.001

Table 2

Somite counts of wildtype and *col* mutants at 16, 27 and 48 hour post fertilization

Hours post fertilization	Number of somites ± 1 SD		P value
	wild-type	*col*	
16	15.5± 0.93 n= 24	14.9± 0.99 n=20	P>0.05
27	30.1± 0.88 n=10	28.7± 1.25 n=10	P< 0.01
48	29.8± 0.63 n=10	28.5± 0.85 n=10	P< 0.01

Table 3

Wnt/PCP components are able to rescue the notochord phenotype in *col* mutant embryos.

Embryos	Notochord diameter-mid trunk (μm)
Uninjected wildtype	40.5±2.5
Uninjected *col* mutants	46.6±2.3
Δ*Ndsh* injected *col* mutants	39.7±3.1
rok2 injected *col* mutants	39.5±3.3
vangl2 injected *col* mutants	40.2±1.6

Table 4

Components of the non-canonical Wnt/PCP pathway can rescue aspects of the *col* mutant phenotype.

RNA constructs	Rescue of body extension	Percentage (%)	Rescue of neuronal migration	Percentage (%)	Total (n)
Δ*Ndsh*	45±5	90	0	0	50
rok2	73.8±6	90	0	0	82
vangl2	40.5±5	90	36±4	80	45

Table 5

hdac1 RNA is able to rescue the *col* mutant phenotype while the *hdac1* MO is able to phenocopy the mutant.

Construct injected	Rescue of CE and neuronal migration defects	Percentage (%)	Mutant phenotype observed	Percentage (%)	*Abnormal	Percentage (%)	Total (n)
hdac1 RNA	106.3±7	85	4±1	3.3	14.7±2	11.7	125
hdac1 MO	0	0	110±5	91.6	10±2	8.3	120

Embryos that displayed severe necrosis and severe loss of head or trunk were classified as ‘abnormal’. Data are from three separate experiments. Homozygous mutants were identified by genotyping. 350pg *hdac1* mRNA was used. Hdac1 MO was injected into wildtype (AB*) embryos.

Table 6

TSA treatment is able to phenocopy the *col* mutant phenotype.

Conc of TSA (nM)	Defects in forebrain development, CE and neuronal migration observed	Percentage (%)	Defects in CE and neuronal migration only observed	Percentage (%)	Total (n)
50 nM at 5 hpf	105	100	0	0	105
800 nM at 16 hpf	0	0	96	100	96